Electronic Supplementary Information

Temperature-dependent hole mobility in pyrene-thiophene-based room-temperature discotic liquid crystals

Shallu Dhingra,[a] *Santosh Prasad Gupta,*[b] *Asmita Shah,*[c] *Dharmendra Pratap Singh*[c] *and Santanu Kumar Pal**[a]

[a] Department of Chemical Sciences, Indian Institute of Science Education and Research (IISER) Mohali, Sector-81, SAS Nagar, Knowledge City, Manauli-140306, India

[b] Department of Physics, Patna University, Patna-800005, India

[c] Université du Littoral Côte d'Opale, UR 4476, UDSMM, Unité de Dynamique et Structure des Matériaux Moléculaires, 62228 Calais cedex, France

*Corresponding author: E-mail: skpal@iisermohali.ac.in; santanupal.20@gmail.com

Contents

1. Materials, Synthesis, and Characterization

1.1. *Methods*

Precursors and solvents required during the synthesis were used as such, available commercially without further alteration. Coupling reactions were carried out in oven-dried flasks using dry solvents and an inert (nitrogen) atmosphere. For the purification of intermediates and final compounds, the column chromatographic technique was adopted using silica gel (100-200 mesh) and neutral alumina gel adsorbents.

The physical methods used are similar to previous reports[1-4] and reproduced here for readers' convenience.

"For structural characterization: ^{1}H NMR (400 MHz) and ^{13}C NMR (100 MHz) in $CDCl_3$ (Bruker Biospin Switzerland Avance-iii), infrared spectroscopy (IR) (attenuated total reflection, Bruker-Alpha), and mass spectrometry (Water Synapt G-2-s QTOF with MALDI ion source and α-cyano-4hydroxy-cinnamic acid as a matrix).

For thermal studies: Differential scanning calorimeter (Perkin Elmer DSC 8000), thermogravimetric analysis (Shimadzu DTG-60 instrument), polarizing optical microscope (Nikon Eclipse LV100POL and a Linkam heating stage (LTS 420)), and X-ray diffraction (Xenocs, GeniX 3D and two-module Pilatus Dectris detector).

For photophysical studies: UV-vis-NIR spectrophotometer (Agilent Technologies, Cary 5000), spectrofluorometer (Horiba Scientific Fluoromax spectrofluorometer), and time-correlated single photon counter (Horiba Jobin Yvon).

For electrochemical and theoretical studies: Cyclic Voltammetry (Princeton Applied Research VersaSTAT) and computational studies (Gaussian 09).

For conductivity studies: Photocurrent curves were recorded on a digital oscilloscope (Keysight, DSOX3022T). A Keysight B2902A Precision Source Measure Unit (SMU) was used to record current-voltage (*I-V*) curves using a Linkam LTS 350 hotplate linked to a Linkam TMS 94 temperature controller. The temperature of the ITO-coated LC cell was maintained during the measurement with an accuracy of ± 0.1 °C."

1.2. Synthesis & characterization

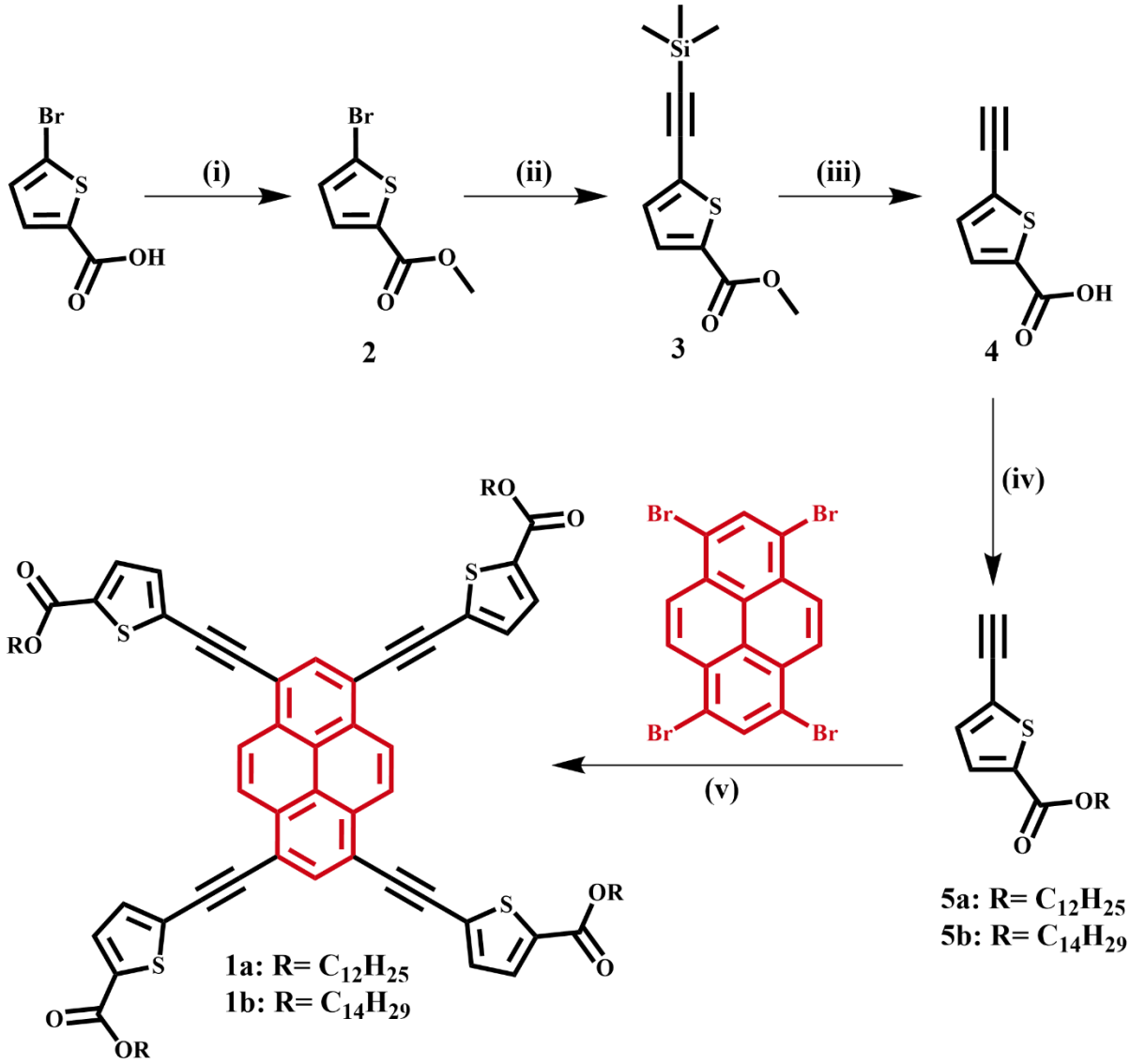

Scheme S1: Reagents and conditions: (i) MeOH, conc. H_2SO_4, reflux, 18 h, yield - 84 %; (ii) TMSA, $PdCl_2(PPh_3)_2$, CuI, NEt_3, RT, 24 h, yield - 81 %; (iii) aq. NaOH (2 N), MeOH, RT, 12 h, yield - 89 %; (iv) aq. KOH (0.1 N), RBr, TOABr, reflux, 18 h, yield - **5a**: 73 %, **5b**: 76%; (v) $Pd(PPh_3)_4$, CuI, DMF/NEt_3, 110 °C, 72 h, yield - **1a**: 41 %, **1b**: 43%.

1.2.1. Procedure for synthesis of tetradodecyl 5,5',5'',5'''-(pyrene-1,3,6,8-tetrayltetrakis(ethyne-2,1-diyl))tetrakis(thiophene-2-carboxylate) (1a)

To an oven-dried 2-neck round bottom flask (RBF), 10 mL dry dimethylformamide (DMF) and 15 mL dry triethylamine (Et_3N) solvents were added with nitrogen purging. After 30 minutes of purging, 1,3,6,8-tetrabromopyrene (140 mg, 0.27 mmol) was added and purged for another 5 minutes. After that, tetrakis(triphenylphosphine)palladium(0) ($Pd(PPh_3)_4$) (31.24 mg,

0.03 mmol) and copper(I) iodide (CuI) (10.30 mg, 0.05mmol) were added to the purging solution. After 10 minutes with continuous purging, compound **5a** (693.17 mg, 2.16 mmol) was added. For 72 hours, the reaction mixture was refluxed at 110 °C while being agitated. The extraction was carried out using diethyl ether organic solvent, and then column chromatography (neutral alumina, 5% EtOAc/hexane) was used for purification to obtain product **1a** as red solid (165.26 mg, yield - 41 %).

^{1}H NMR ($CDCl_3$, 400 MHz, δ ppm): 8.54 (4H, s), 8.33 (2H, s), 7.73 (4H, d), 7.37 (4H, d), 4.33 (8H, m), 1.82-1.75 (8H, m), 1.50-1.42 (8H, m), 1.40-1.25 (64H, m), 0.87 (12H, t).

^{13}C NMR ($CDCl_3$, 100 MHz, δ ppm): 161.71, 135.19, 133.21, 132.95, 132.79, 130.96, 129.63, 126.35, 122.58, 117.95, 93.87, 89.32, 65.96, 32.29, 30.07, 30.04, 30.02, 29.99, 29.74, 29.72, 29.07, 26.35, 23.06, 14.49.

HRMS (MALDI) m/z: $[M+H]^+$: 1475.7475 (Theoretical), 1475.7495 (Observed).

IR (ATR, cm^{-1}): 2954, 2922, 2853, 2186, 1713, 1599, 1527, 1494, 1448, 1380, 1342, 1278, 1237, 1184, 1099, 1027, 970, 889, 824, 743, 717, 658, 638, 580, 559, 533.

1.2.2. Procedure for synthesis of tetrakis(tetradecyl) 5,5',5'',5'''-(pyrene-1,3,6,8-tetrayltetrakis(ethyne-2,1-diyl))tetrakis(thiophene-2-carboxylate) (1b)

With nitrogen purging, 10 mL of dry DMF and 15 mL of dry Et_3N solvents were poured into a oven-dried 2-neck RBF. After 30 minutes of purging, 140 mg of 1,3,6,8-tetrabromopyrene (0.27 mmol) was introduced and purged for five minutes. After that, $Pd(PPh_3)_4$ (31.24 mg, 0.03 mmol) and CuI (10.30 mg, 0.05 mmol) were added to the purging solution. After 10 minutes with continuous purging, compound **5b** (753.84 mg, 2.16 mmol) was added. For 72 hours, the reaction mixture was refluxed at 110 °C while being agitated. The extraction was carried out using diethyl ether organic solvent. Then column chromatography (neutral alumina, 5% EtOAc/hexane) was used to purify product **1b** as red solid (184.66 mg, yield - 43 %).

^{1}H NMR ($CDCl_3$, 400 MHz, δ ppm): 8.63 (4H, s), 8.40 (2H, s), 7.75 (4H, d), 7.40 (4H, d), 4.33 (8H, m), 1.82-1.75 (8H, m), 1.47-1.42 (8H, m), 1.40-1.25 (80H, m), 0.86 (12H, t).

^{13}C NMR ($CDCl_3$, 100 MHz, δ ppm): 161.76, 135.28, 133.29, 133.13, 132.86, 131.20, 129.63, 126.56, 122.90, 118.10, 93.88, 89.37, 65.99, 32.28, 30.09, 30.04, 30.03, 29.98, 29.73, 29.72, 29.08, 26.35, 23.05, 14.48.

HRMS (MALDI) m/z: $[M+H]^+$: 1587.8727 (Theoretical), 1587.8745 (Observed).

IR (ATR, cm^{-1}): 2955, 2919, 2851, 2188, 1712, 1599, 1527, 1493, 1449, 1379, 1344, 1253, 1172, 1096, 1026, 1000, 951, 887, 817, 745, 679, 598, 573, 538, 515.

1.2.3. Procedure for synthesis of methyl 5-bromothiophene-2-carboxylate (2)

The procedure followed is similar to the reported one, with slight modifications.[5]
The precursor 5-bromo-2-thiophene carboxylic acid (5 g, 24.15 mmol) was added to 50 mL methanol (MeOH) and 2 mL concentrated H_2SO_4 in a 100 mL RBF. For 18 hours, the reaction mixture was refluxed. Next, a rotary evaporator (rotavap) was used to extract the MeOH solvent. Compound **2** (4.49 g, yield - 84 %) was obtained as a white solid from the remaining residue by column chromatography (silica gel 100-200 mesh, hexane).

^{1}H NMR ($CDCl_3$, 400 MHz, δ ppm): 7.54 (1H, d), 7.06 (1H, d), 3.87 (3H, s).

^{13}C NMR ($CDCl_3$, 100 MHz, δ ppm): 161.52, 134.75, 133.77, 131.01, 120.33, 52.38.

IR (ATR, cm^{-1}): 2992, 2945, 2842, 1713, 1532, 1438, 1413, 1331, 1255, 1190, 1093, 1049, 972, 954, 811, 787, 740, 658, 546, 505.

1.2.4. Procedure for synthesis of methyl 5-((trimethylsilyl)ethynyl)thiophene-2-carboxylate (3)

In a 100 mL two-necked RBF, dry Et_3N was taken and purged for 20 minutes. Compound **2** (4.00 g, 18.09 mmol), $PdCl_2(PPh_3)_2$ (127.0 mg, 180.94 μmol), and CuI (51.7 mg, 271.41 μmol) were added to the purged solvent in that order. After that, trimethylsilylacetylene (TMSA) (2.7 g, 27.14 mmol) was added, and the reaction mixture was allowed to stir for 24 hours at room temperature. Diethyl ether was used to extract the reaction mixture after using 10 % aqueous HCl to neutralize the reaction mixture. After drying over sodium sulfate, the organic layer was concentrated in the rotavap. Utilizing column chromatography (silica gel 100-200 mesh, hexane) for purification, compound **3** (3.51 g, yield – 81 %) was obtained as a brown solid.

^{1}H NMR ($CDCl_3$, 400 MHz, δ ppm): 7.62 (1H, d), 7.15 (1H, d), 3.88 (3H, s), 0.26 (9H, s).

^{13}C NMR ($CDCl_3$, 100 MHz, δ ppm): 162.16, 134.07, 133.31, 133.06, 130.03, 102.29, 96.87, 52.59, -0.05.

IR (ATR, cm^{-1}): 2953, 2899, 2844, 2147, 1714, 1526, 1443, 1335, 1289, 1249, 1190, 1095, 957, 840, 741, 702, 649, 575, 535, 508.

1.2.5. Procedure for synthesis of 5-ethynylthiophene-2-carboxylic acid (4)

To the methanolic solution of compound **3** (3 g, 12.58 mmol), 2 N NaOH (aq.) (12.58 mL, 25.17 mmol) was added. For 12 hours, the reaction was agitated at room temperature. A 10 % HCl solution was used to acidify the reaction mixture before the product was extracted using dichloromethane (DCM) organic solvent. Following rotavap distillation, the organic layer was passed through sodium sulfate to get the final product **4** (1.71 g, yield – 89 %) as a brown solid.

^{1}H NMR ($CDCl_3$, 400 MHz, δ ppm): 7.73 (1H, d), 7.24 (1H, d), 5.15 (1H, br), 3.50 (1H, s).

^{13}C NMR ($CDCl_3$, 100 MHz, δ ppm): 166.93, 134.86, 133.86, 133.82, 130.45, 84.77, 76.35.

IR (ATR, cm^{-1}): 3286, 3101, 2815, 2662, 2535, 2150, 1667, 1524, 1449, 1418, 1334, 1310, 1278, 1238, 1135, 1110, 1033, 931, 912, 832, 749, 689, 654, 624, 524, 508.

1.2.6. Procedure for synthesis of dodecyl 5-ethynylthiophene-2-carboxylate (5a)

A solution of 0.1 N KOH (aq.) (60.46 mL, 6.04 mmol) was used to dissolve compound **4** (800 mg, 5.26 mmol). 1-bromododecane (2.52 mL, 10.51 mmol) was added after the addition of a catalytic quantity of tetraoctylammonium bromide (TOABr). For 18 hours, the reaction mixture was refluxed. Compound **5a** (1.23 g, yield - 73 %) was obtained by purifying the crude product using column chromatography (silica gel 100-200 mesh, hexane) after it was extracted using a DCM organic solvent.

^{1}H NMR ($CDCl_3$, 400 MHz, δ ppm): 7.63 (1H, d), 7.21 (1H, d), 4.28 (2H, t), 3.44 (1H, s), 1.76-1.69 (2H, m), 1.43-1.26 (18H, m), 0.88 (3H, t)

^{13}C NMR ($CDCl_3$, 100 MHz, δ ppm): 161.62, 135.12, 133.45, 132.97, 128.56, 83.88, 76.48, 65.83, 32.20, 29.93, 29.85, 29.80, 29.64, 29.51, 28.90, 26.20, 22.97, 14.39.

IR (ATR, cm^{-1}): 3307, 2924, 2854, 2145, 1712, 1526, 1443, 1382, 1335, 1280, 1249, 1217, 1095, 1032, 950, 820, 748, 721, 694, 659, 608, 577, 561, 528, 508.

1.2.7. Procedure for synthesis of tetradecyl 5-ethynylthiophene-2-carboxylate (5b)

A solution of 0.1 N KOH (aq.) (60.46 mL, 6.04 mmol) was used to dissolve compound **4** (800 mg, 5.26 mmol). 1-bromotetradecane (3.13 mL, 10.51 mmol) was added after the addition of a catalytic quantity of tetraoctylammonium bromide (TOABr). For 18 hours, the reaction mixture was refluxed. Compound **5b** (1.39 g, yield - 76 %) was obtained by purifying the crude

product using column chromatography (silica gel 100-200 mesh, hexane) after it was extracted using a DCM organic solvent.

^{1}H NMR ($CDCl_3$, 400 MHz, δ ppm): 7.63 (1H, d), 7.21 (1H, d), 4.28 (2H, t), 3.44 (1H, s), 1.76-1.69 (2H, m), 1.42-1.25 (22H, m), 0.88 (3H, t)

^{13}C NMR ($CDCl_3$, 100 MHz, δ ppm): 161.61, 135.13, 133.45, 132.96, 128.56, 83.89, 76.48, 65.83, 32.22, 29.99, 29.97, 29.96, 29.86, 29.80, 29.66, 29.52, 28.91, 26.21, 22.98, 14.40.

IR (ATR, cm^{-1}): 3312, 2925, 2854, 2142, 1717, 1527, 1444, 1382, 1336, 1281, 1252, 1218, 1097, 1035, 942, 873, 821, 750, 722, 694, 662, 606, 570, 544, 523.

2. NMR Spectra

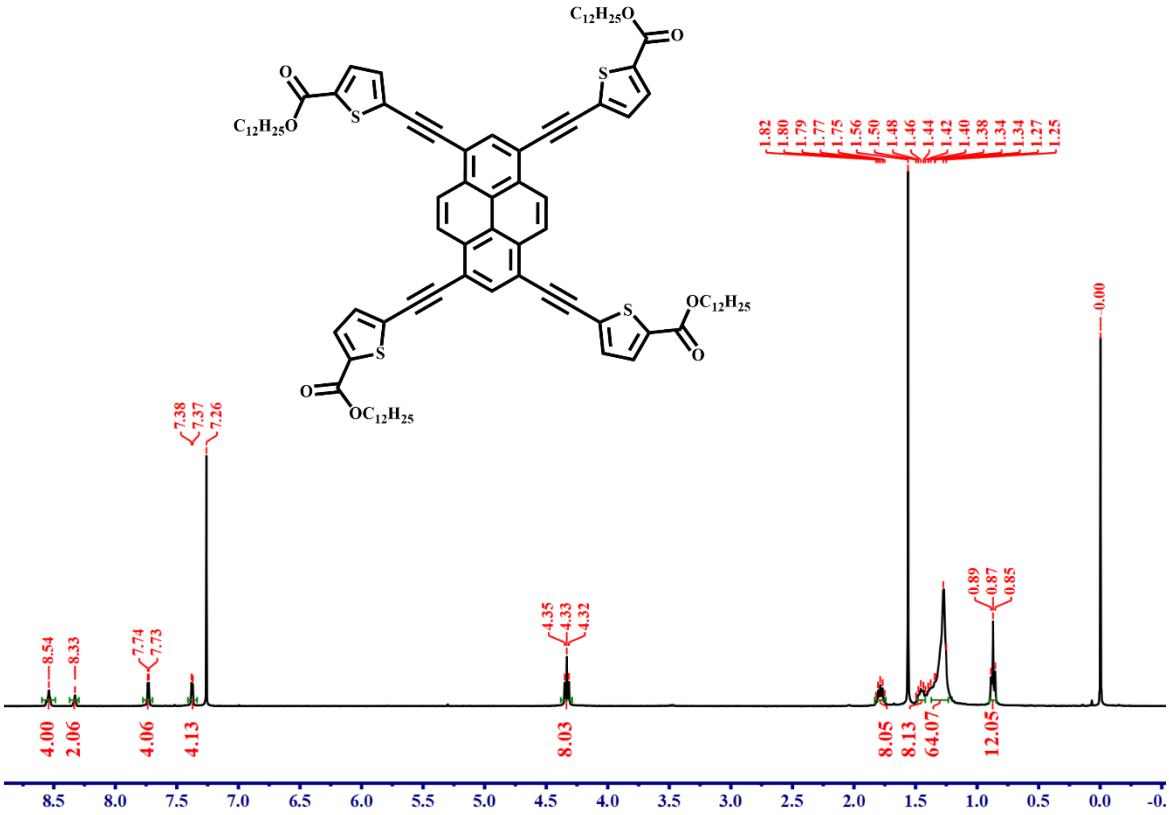

Figure S1. ^{1}H NMR of compound **1a**.

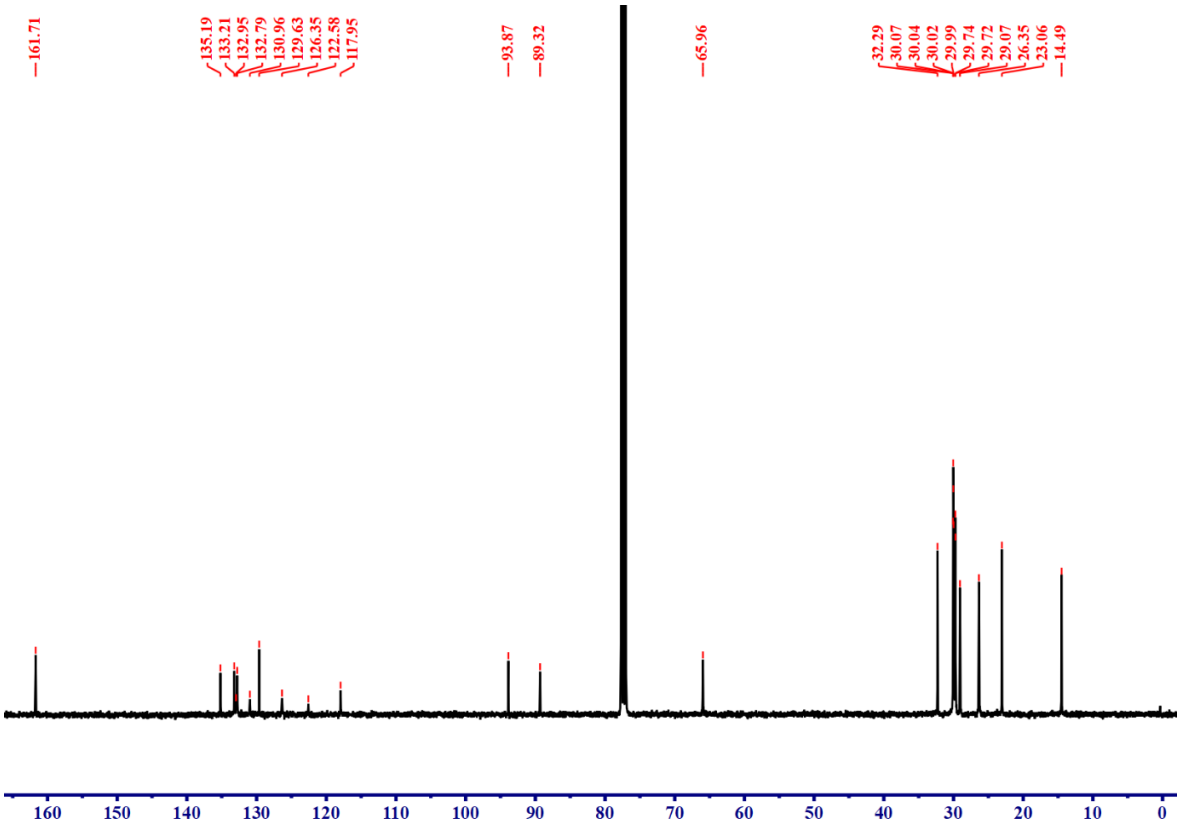

Figure S2. ^{13}C NMR of compound **1a**.

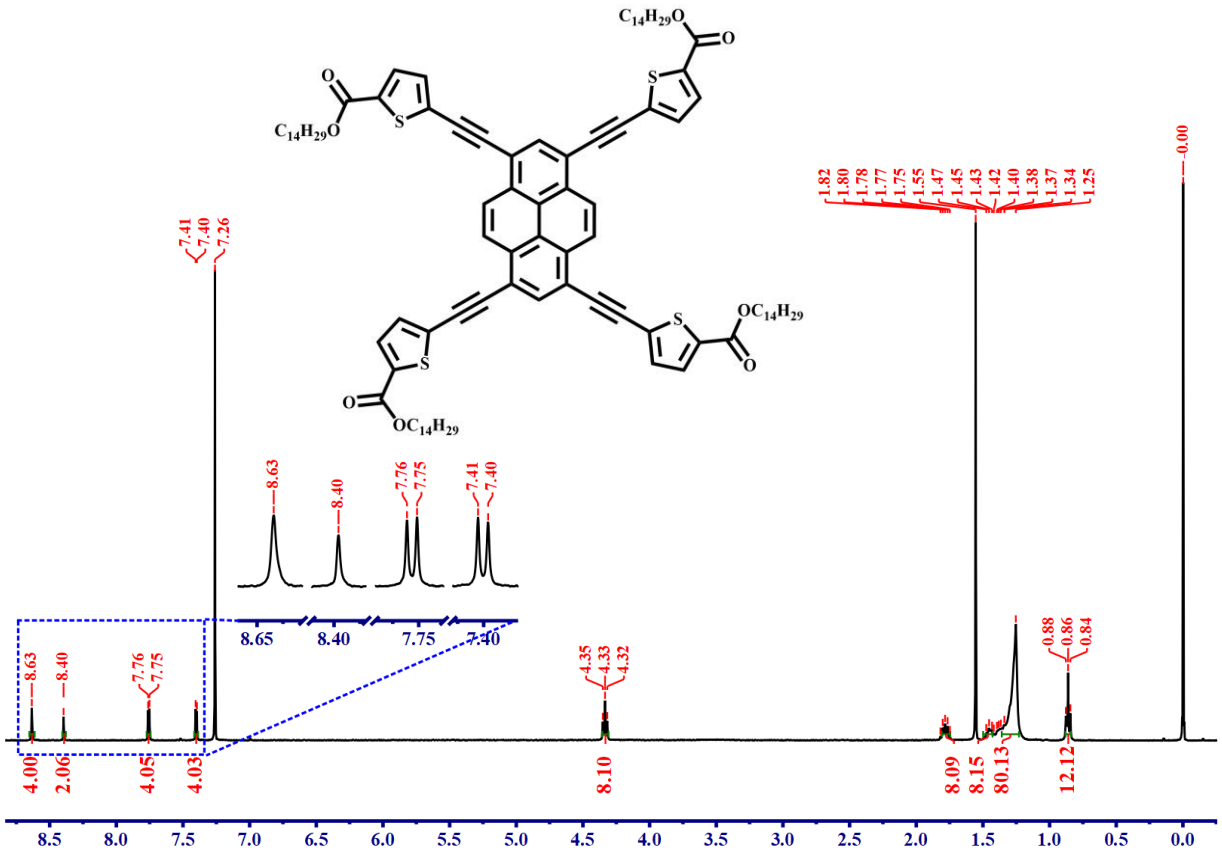

Figure S3. ^{1}H NMR of compound **1b**.

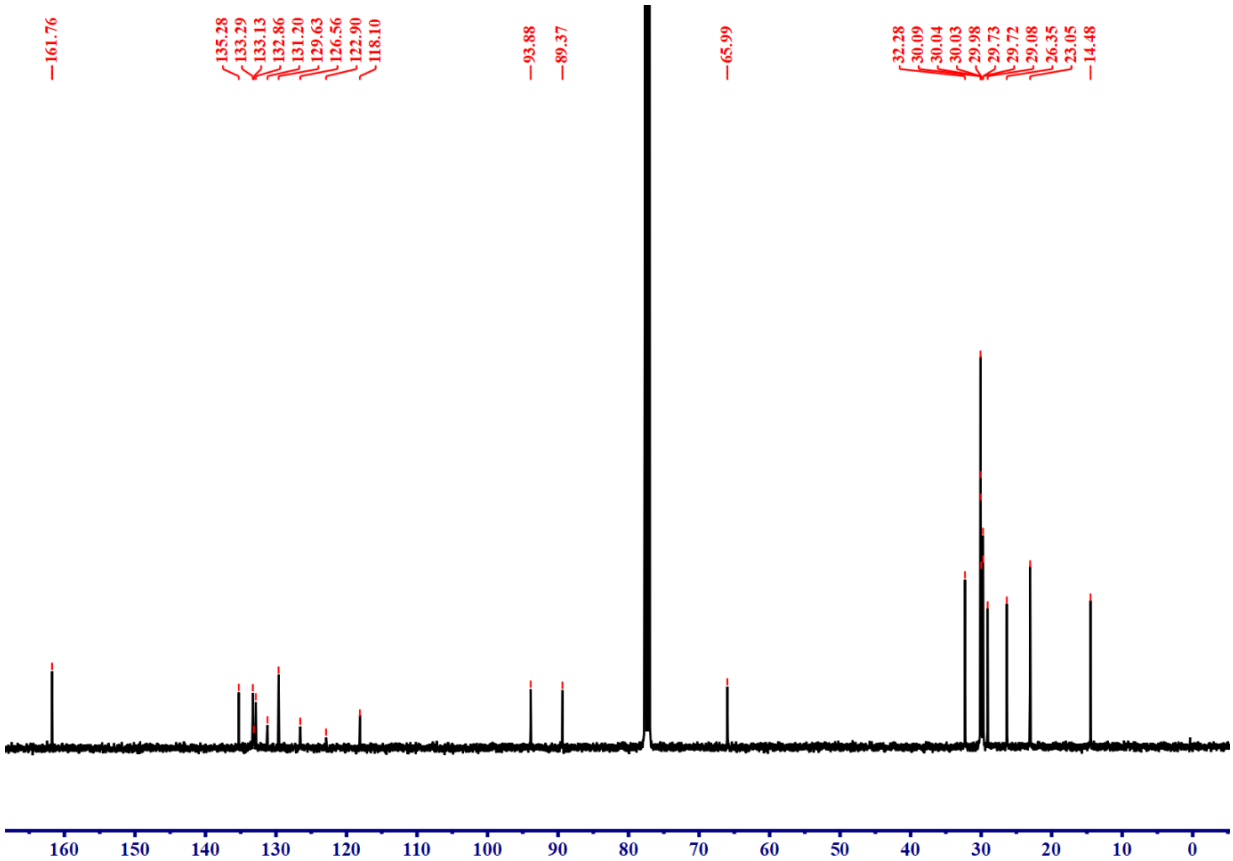

Figure S4. ^{13}C NMR of compound **1b**.

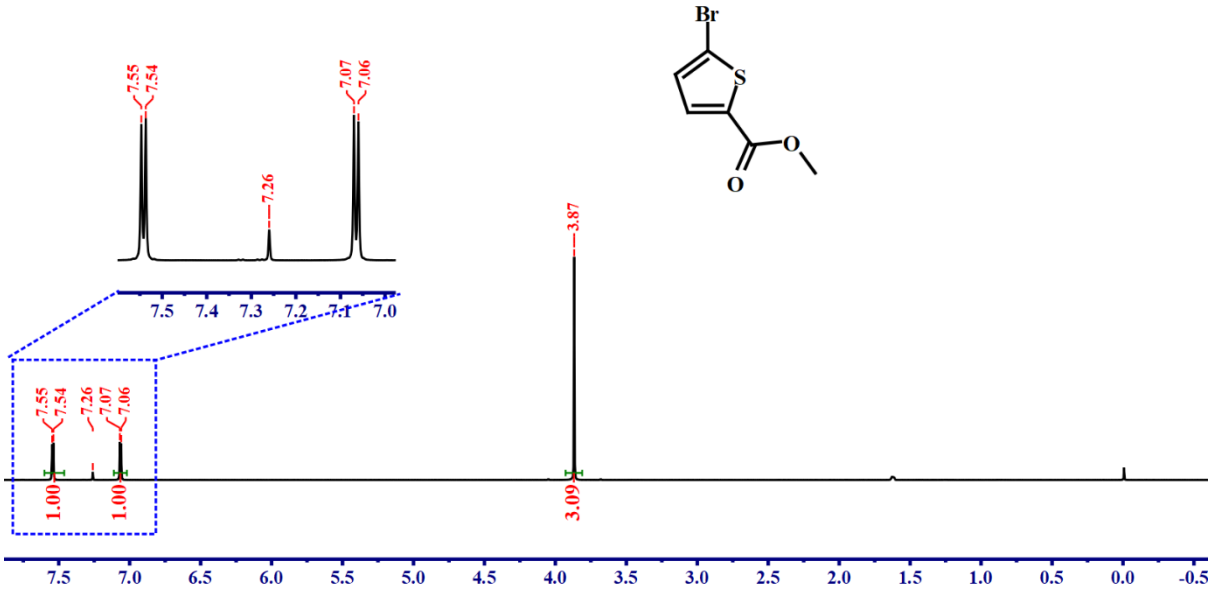

Figure S5. ^{1}H NMR of compound **2**.

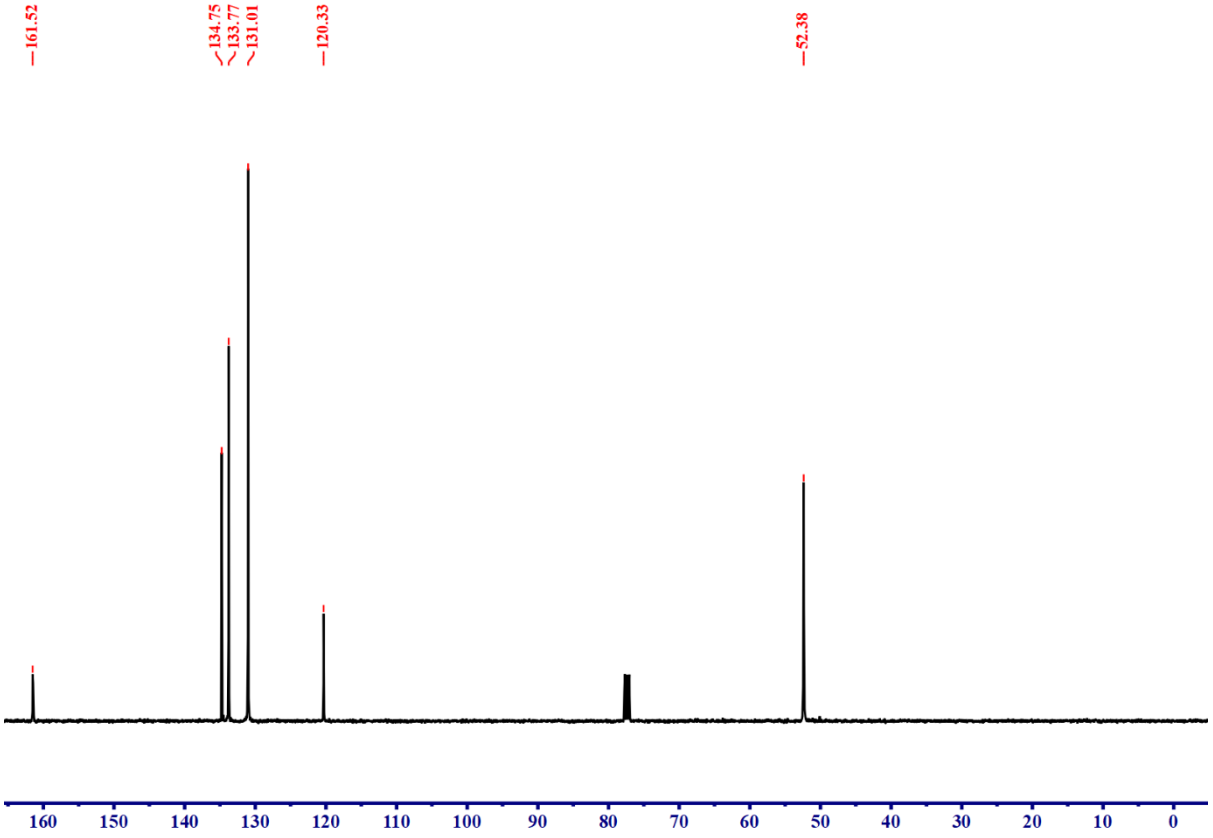

Figure S6. ^{13}C NMR of compound **2**.

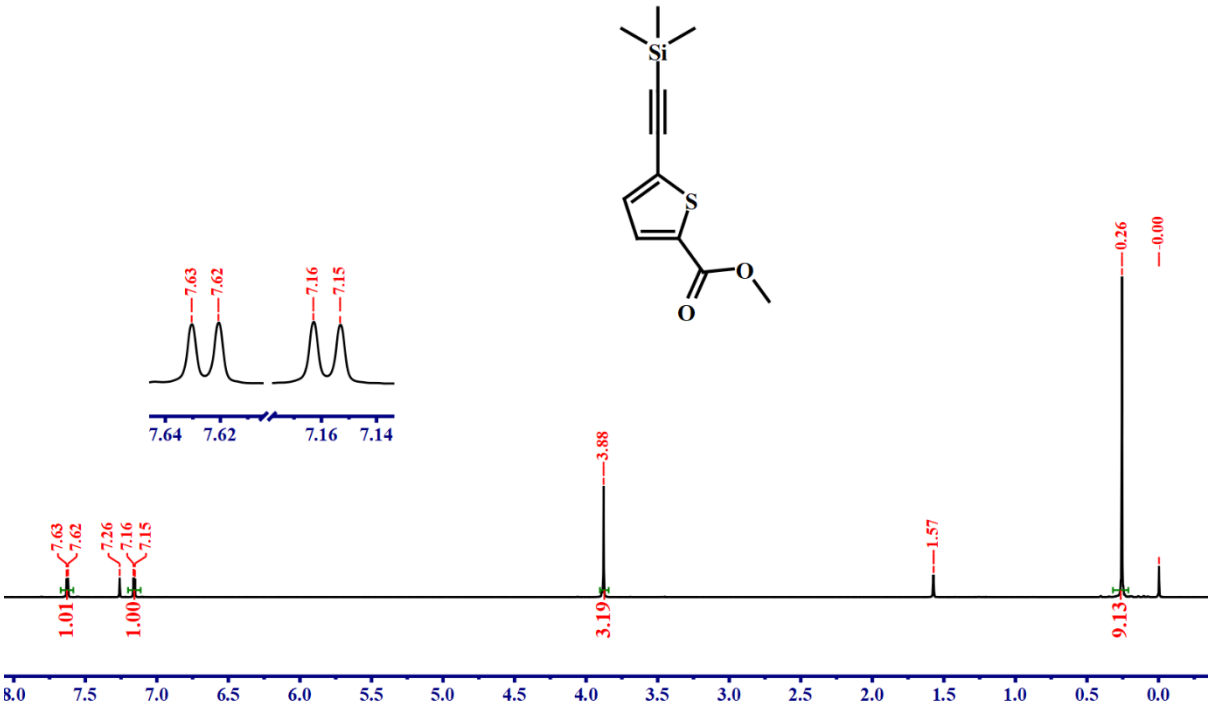

Figure S7. ^{1}H NMR of compound **3**.

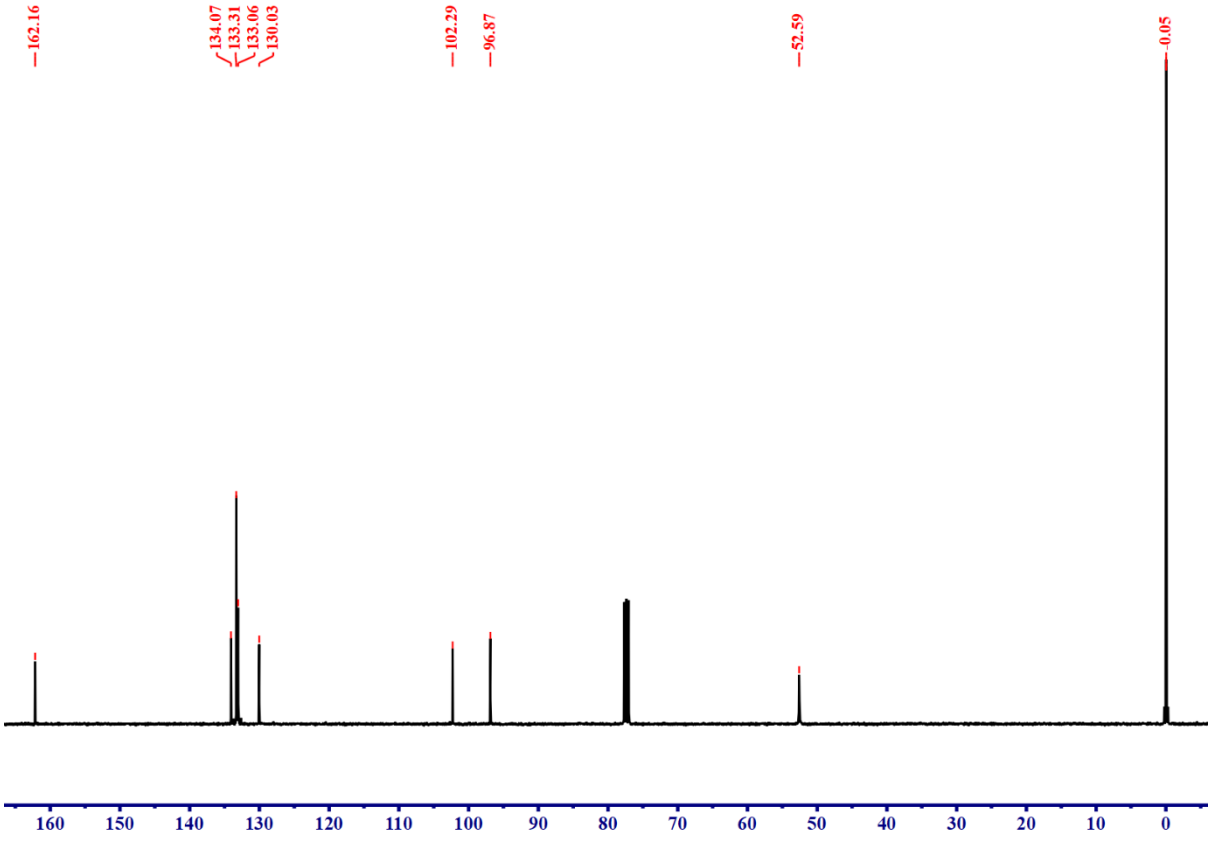

Figure S8. ^{13}C NMR of compound **3**.

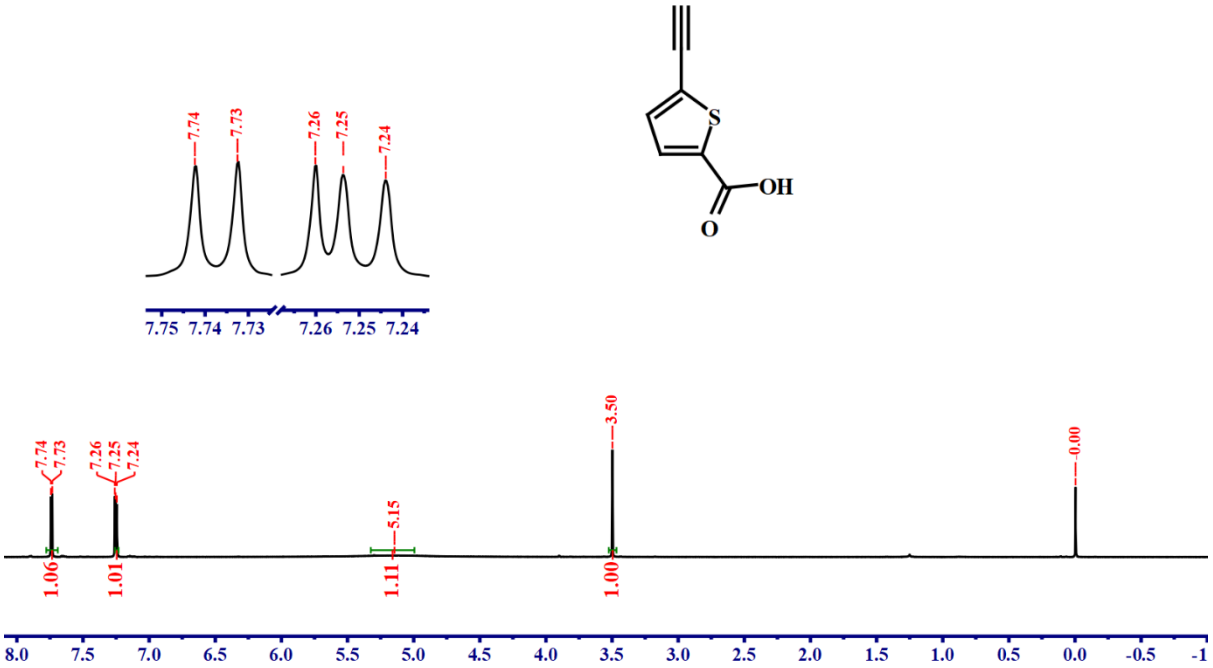

Figure S9. ^{1}H NMR of compound **4**.

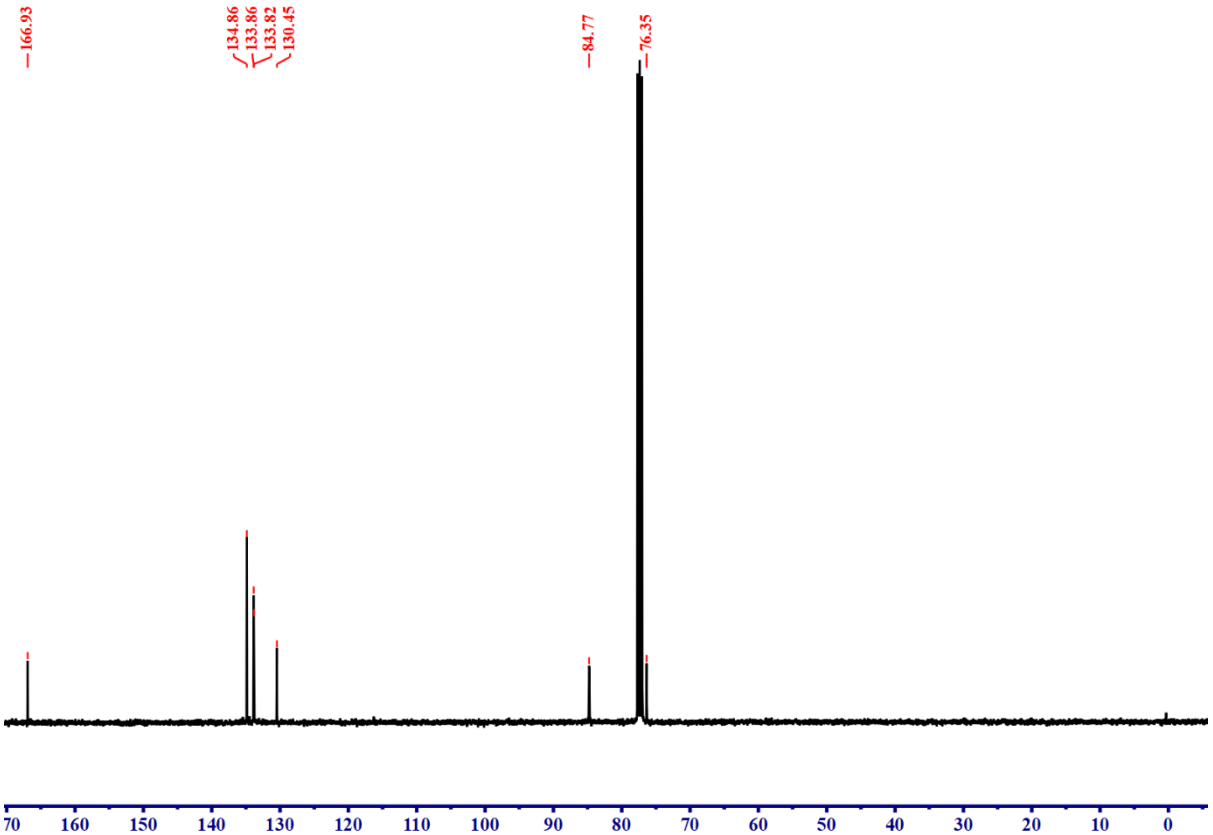

Figure S10. ^{13}C NMR of compound **4**.

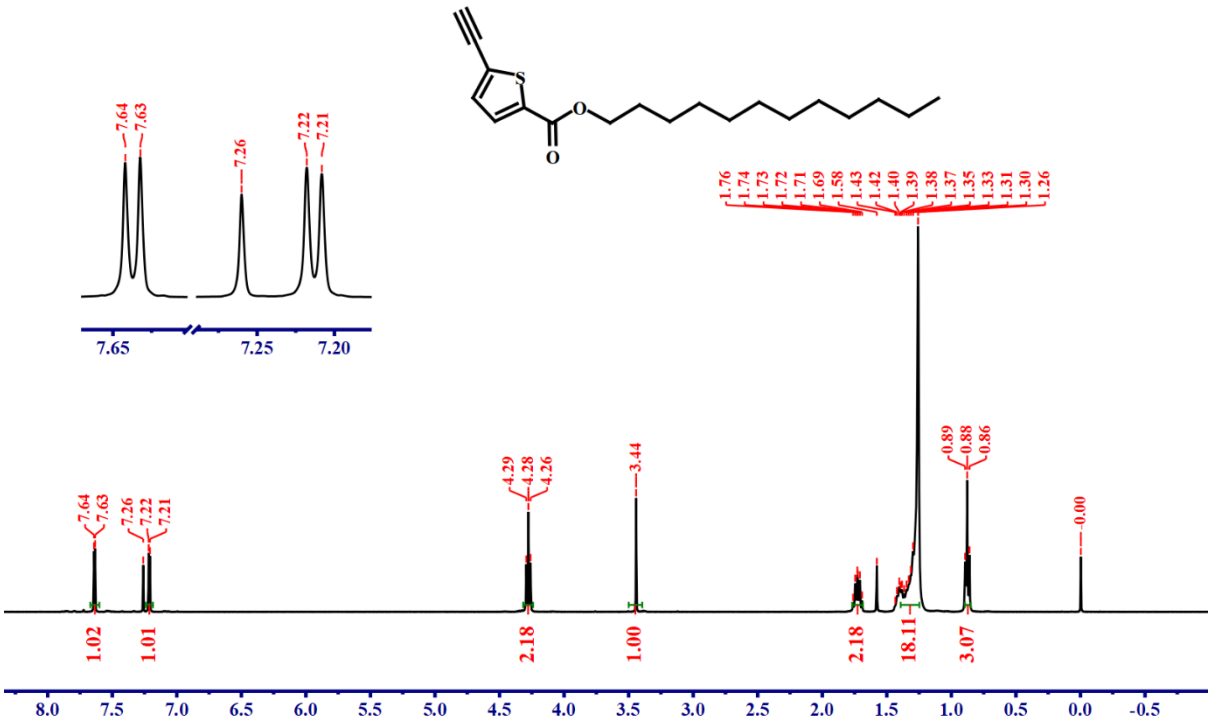

Figure S11. ^{1}H NMR of compound **5a**.

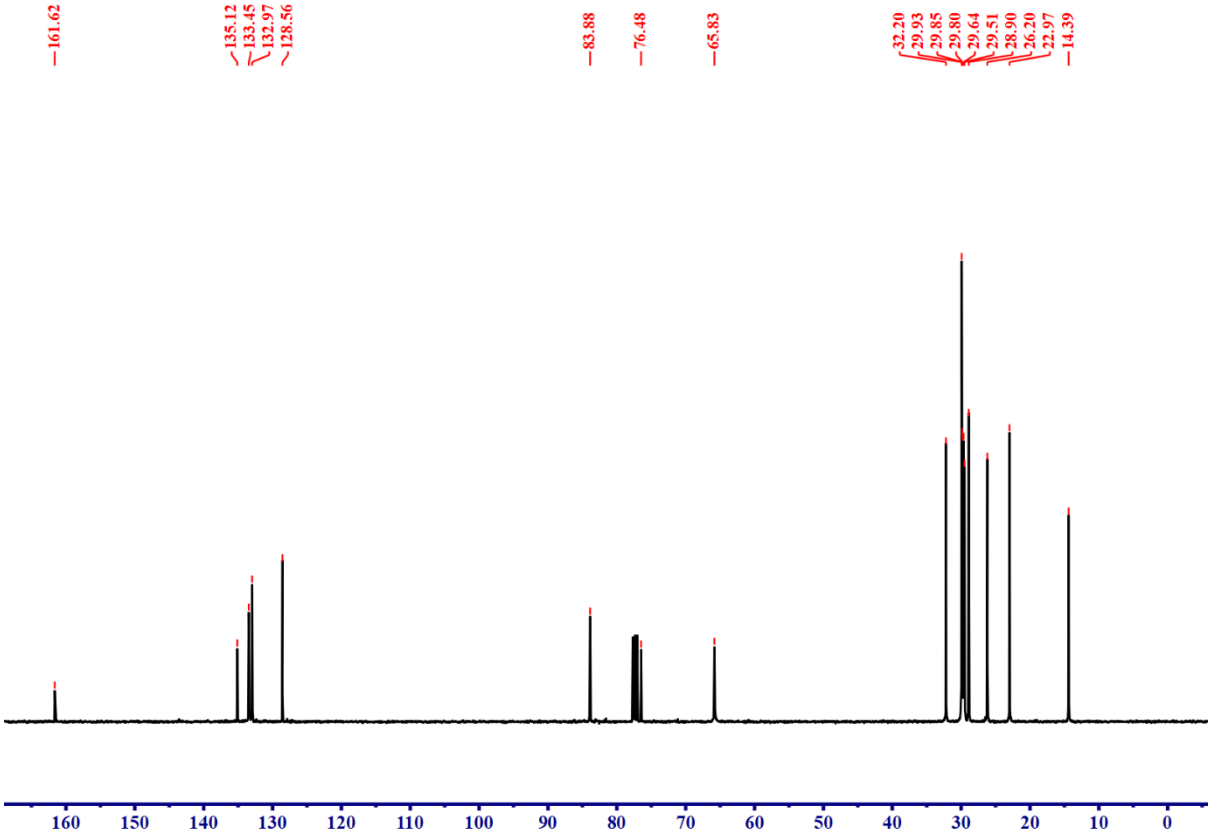

Figure S12. ^{13}C NMR of compound **5a**.

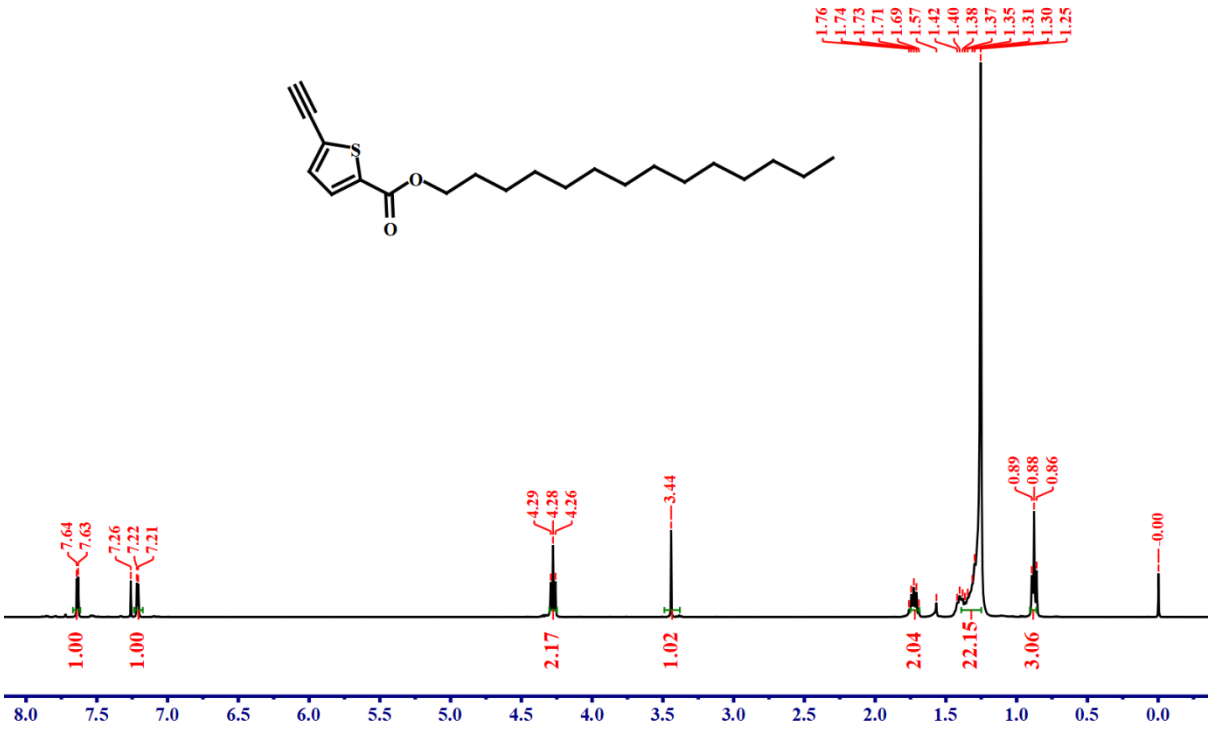

Figure S13. ^{1}H NMR of compound **5b**.

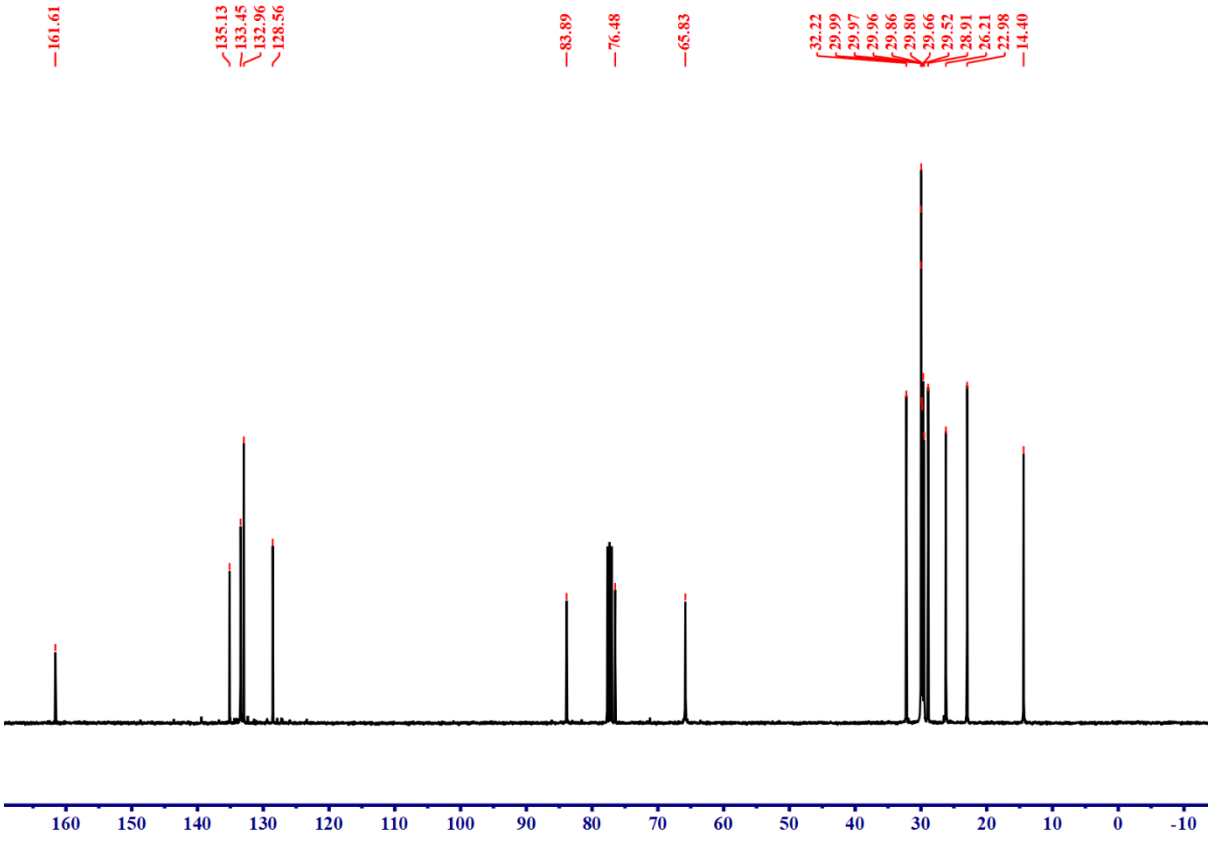

Figure S14. ^{13}C NMR of compound **5b**.

3. HRMS Spectra

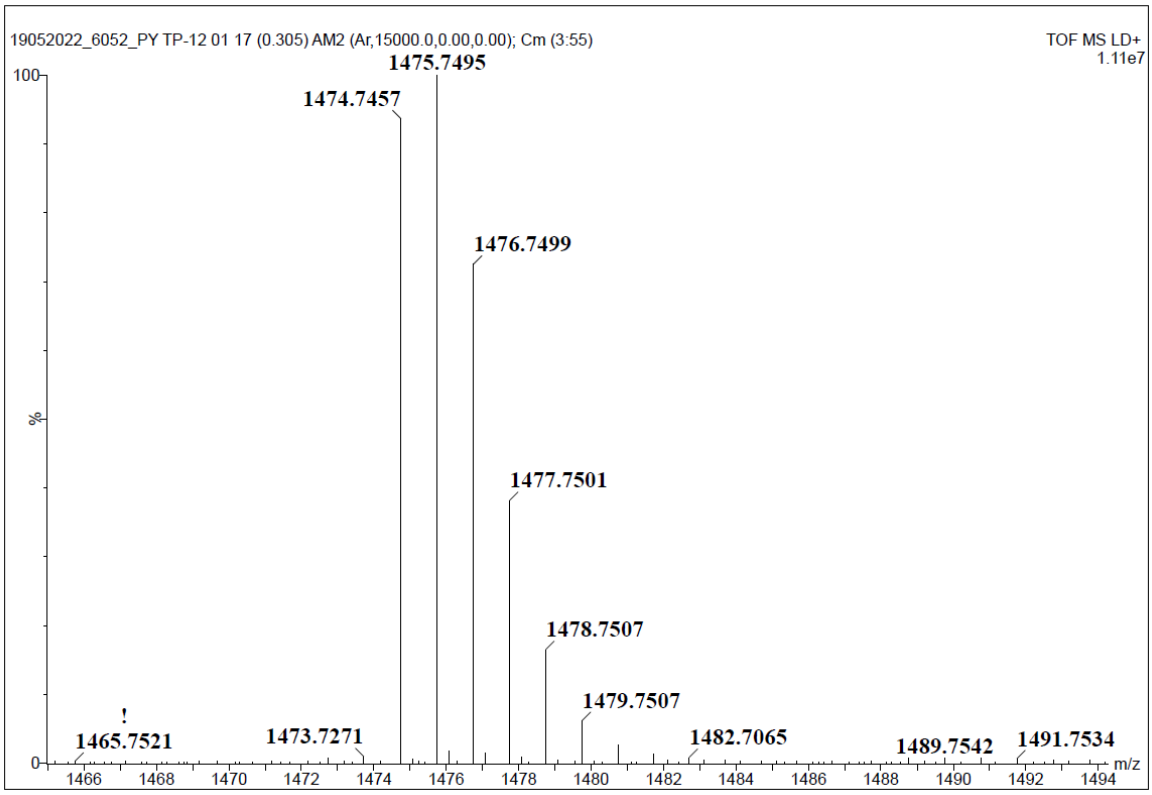

Figure S15. HRMS Data for compound **1a**.

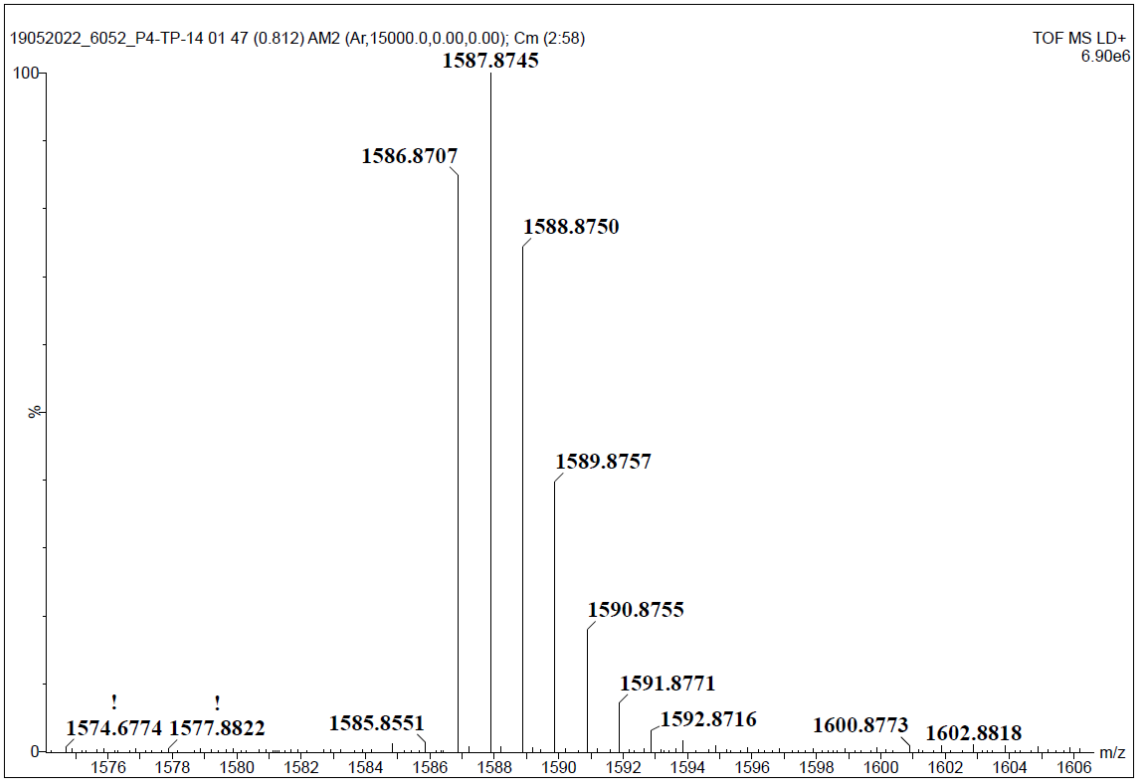

Figure S16. HRMS Data for compound **1b**.

4. Thermal Studies

4.1. *Polarized Optical Microscopic (POM) Images*

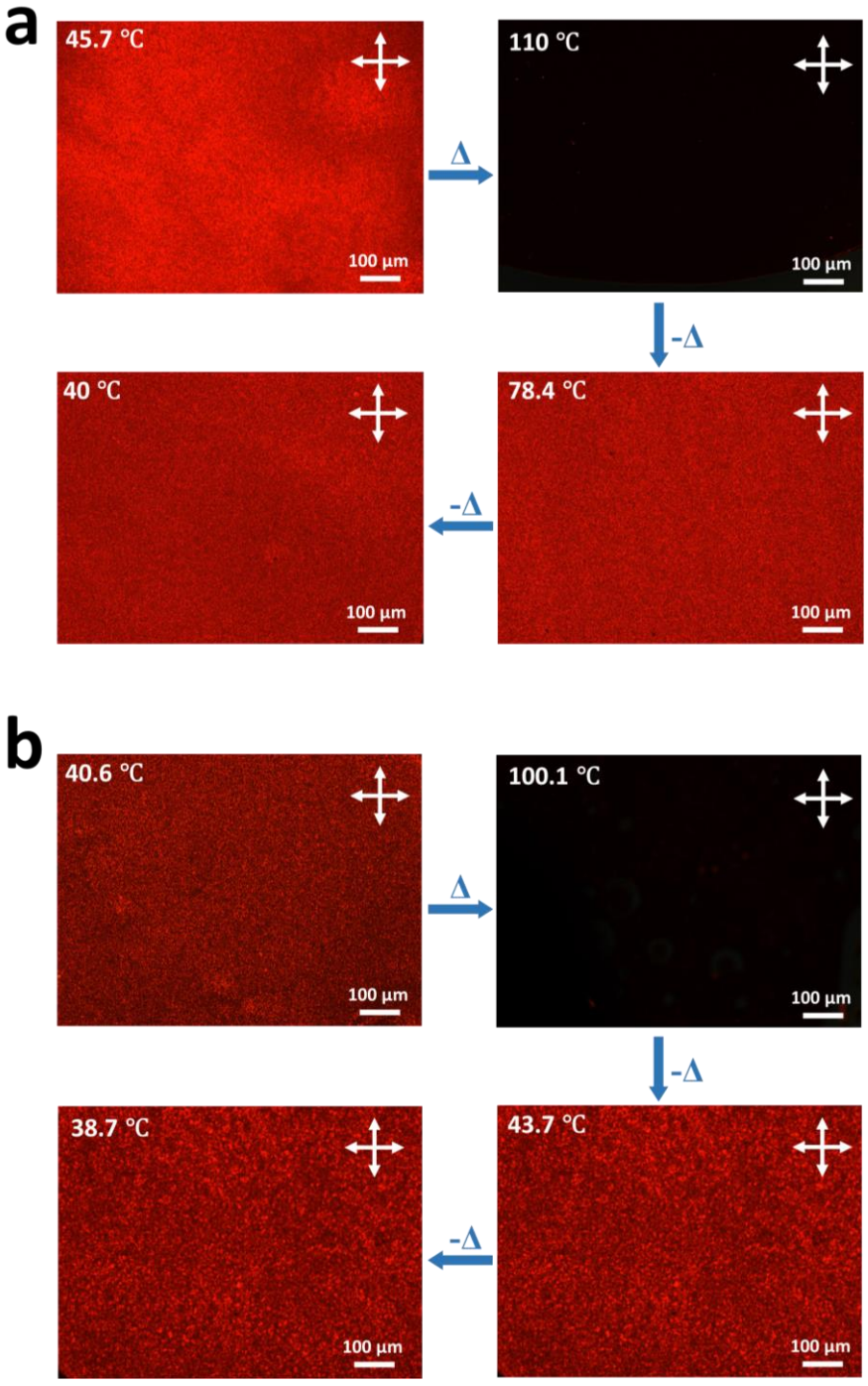

Figure S17. POM textures recorded for (a) compound **1a** and (b) compound **1b** under a crossed polarizer during heating and cooling.

4.2. Differential Scanning Calorimetry (DSC) Thermograms

Table S1: Thermal data for mesogens **1a** and **1b** showing phase transitions temperatures and enthalpy (in parentheses) detected from DSC.	
Mesogen	**Heating / cooling °C (kJ mol^{-1})**
1a	Cr -19.4 (10.9) Col_{ob} 99.9 (8.7) Iso / Iso 82.9 (7.7) Col_{ob} -26.8 (23.2) Cr
1b	Cr -8.9 (9.8) Col_{ob} 71.9 (2.4) Iso / Iso 54.1 (2.2) Col_{ob} -13.7 (6.2) Cr
Abbreviations: Cr - crystalline phase, Col_{ob} - columnar oblique phase, and Iso - isotropic phase.	

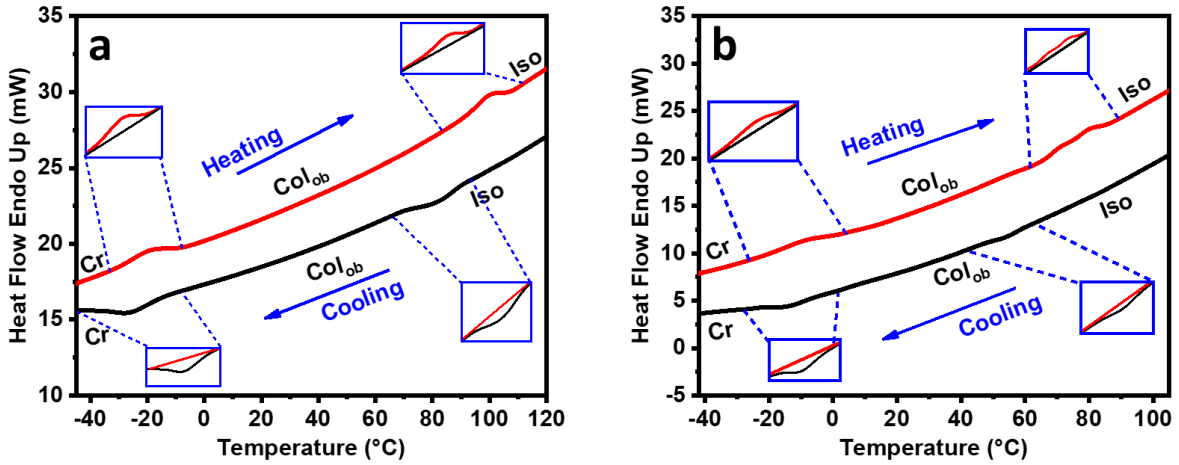

Figure S18. DSC thermal profile recorded with a scan rate of 10 °C/min for compounds (a) **1a** and (b) **1b**.

4.3. ***Thermogravimetric Analysis (TGA) Curves***

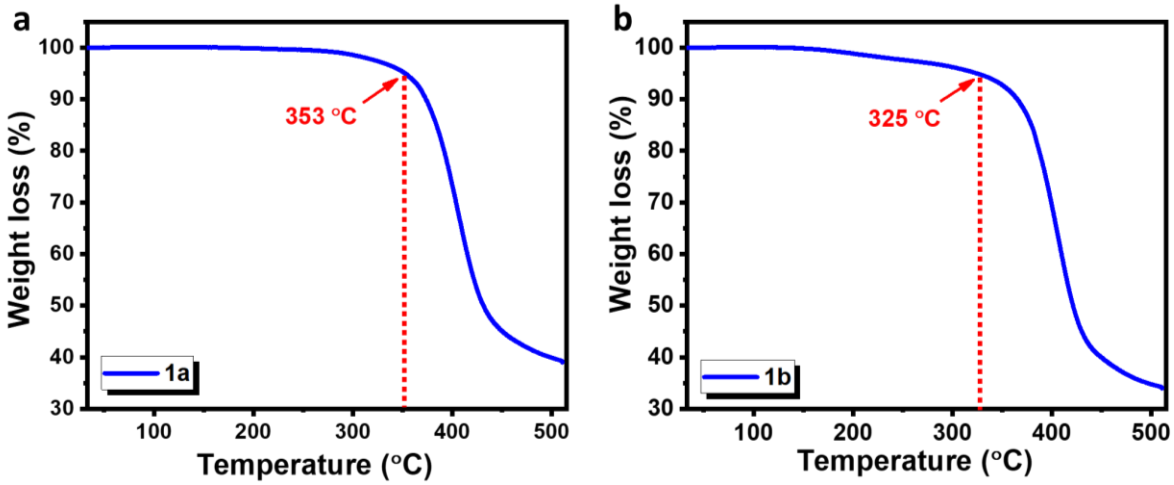

Figure S19. TGA data for compounds (a) **1a** and (b) **1b** under nitrogen environment obtained at a 10 °C/min heating rate. The figure shows the temperature at which 5% of weight was lost.

4.4. *X-ray Diffraction (XRD) Studies*

Table S2: Indexing of the observed peaks for compound **1a** on the 2-dimensional oblique lattice. The *d*-spacings are calculated as: $\boldsymbol{d_{cal}} = \frac{\sin(\alpha)}{\sqrt{\frac{h^2}{a^2} + \frac{k^2}{b^2} - \frac{2h\,k\cos(\alpha)}{a\,b}}}$, where *a*, *b*, and α are the lattice parameters of the unit cell and (*hk*) is the Miller indices of the reflecting planes. The lattice parameters are *a* = 75.98 Å, *b* = 72.29 Å & α = 69.06˚

(*hk*)	d_{exp} (Å)	d_{cal} (Å)	*Relative intensity I*(*hk*)	*Multiplicity*	*Phase Φ*(*hkl*)
(20)	35.48	35.48	100.00	2	0
(02)	33.76	33.76	29.66	2	0
(22)	30.50	30.50	48.64	2	0
(-21)	27.44	27.61	//	//	//
(31)	25.70	25.33	7.61	2	π
(30)	23.44	23.65	5.11	2	π
(03)	22.53	22.50	//	//	//
(33)	20.49	20.33	1.82	2	π
(-13)	19.54	19.53	//	//	//
(40)	17.76	17.74	1.48	2	0
(43)	17.45	17.25			
(34)	16.96	16.89			
(-23)	16.34	16.52			
(57)	9.81	9.76			
(76)	9.33	9.38			
(68)	8.35	8.44			
(97)	7.39	7.57			
h_a	5.05	Fluid alkyl chain-chain correlations			
(11 16)	4.30	4.31			
(15 14)	4.21	4.21			
h_c	3.80	Core-core separation			
(14 18)	3.70	3.72			

Table S3: Indexing of the observed peaks for compound **1b** on the 2-dimensional oblique lattice. The *d*-spacings are calculated as: $\boldsymbol{d_{cal} = \frac{\sin(\alpha)}{\sqrt{\frac{h^2}{a^2} + \frac{k^2}{b^2} - \frac{2h\,k\cos(\alpha)}{a\,b}}}}$, where *a*, *b*, and α are the lattice parameters of the unit cell and (*hk*) is the Miller indices of the reflecting planes. The lattice parameters are *a* = 76.33 Å, *b* = 68.62 Å & α = 71.89˚

(hk)	$\boldsymbol{d_{exp}}$ **(Å)**	$\boldsymbol{d_{cal}}$ **(Å)**	***Relative intensity I(hk)***	***Multiplicity***	***Phase Φ(hkl)***
(20)	36.27	36.27	100.00	2	0
(02)	32.61	32.61	48.07	2	0
(22)	29.08	29.18	12.53	2	0
(-12)	26.55	26.79	3.70	2	π
(31)	25.33	25.39	2.80	2	0
(32)	23.17	23.18	2.07	2	0
(03)	21.63	21.74	2.25	2	π
(41)	19.01	19.07	//	//	//
(40)	18.30	18.14			
(04)	16.67	16.30			
(35)	13.38	13.34			
(74)	10.46	10.32			
(66)	9.52	9.72			
(86)	8.28	8.36			
$\mathbf{h_a}$	5.05	Fluid alkyl chain-chain correlations			
$\mathbf{h_c}$	3.82	Core-core separation			

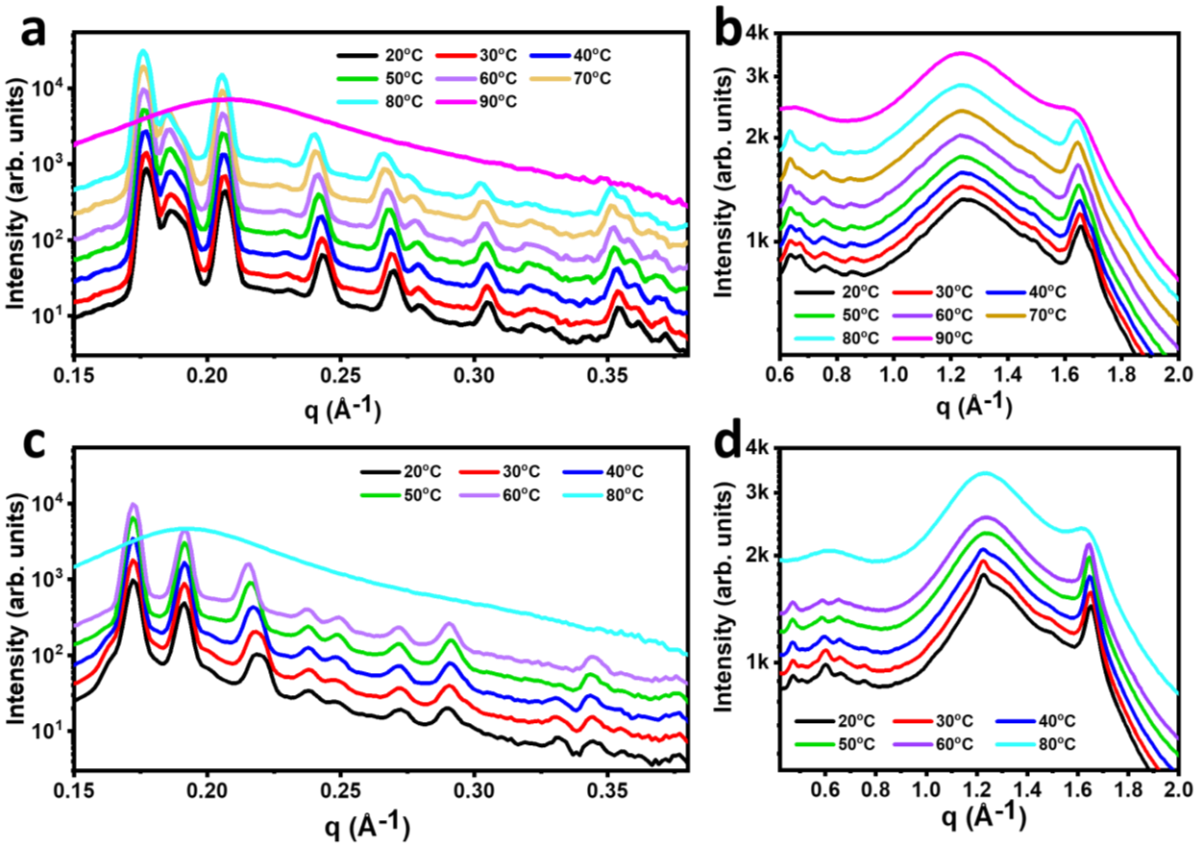

Figure S20. Variation in (a) small-angle and (b) wide-angle XRD pattern of compound **1a** with temperature. Variation in (c) small-angle and (d) wide-angle XRD pattern of compound **1b** with temperature.

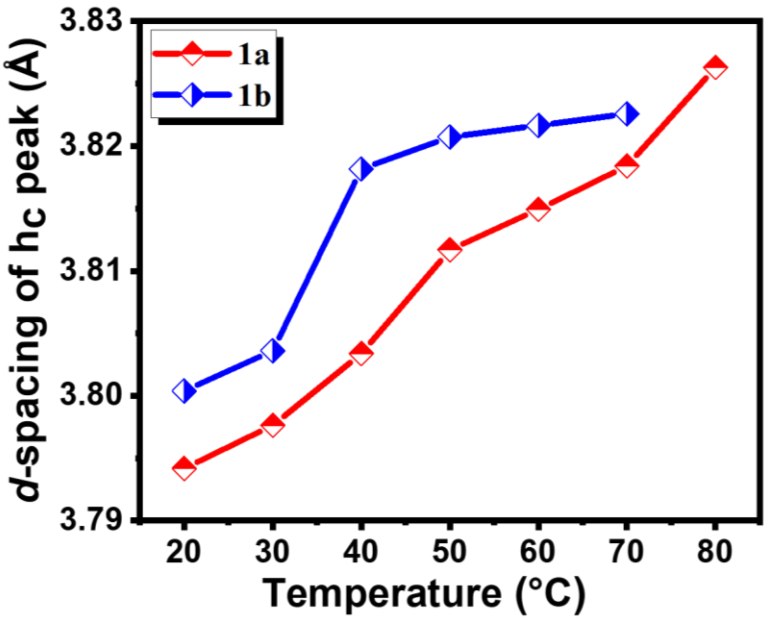

Figure S21. Variation of core–core separation (h_c peak *d*-spacing) of compound **1a** (half-filled diamond in red color) and compound **1b** (half-filled diamond in blue color) with temperature.

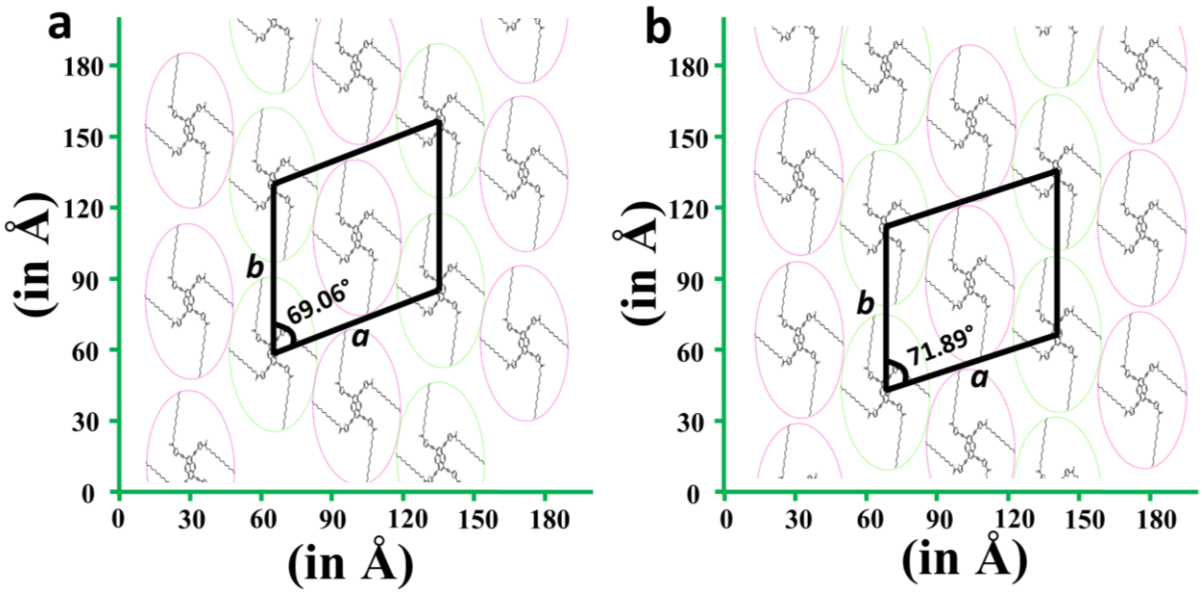

Figure S22: 2-D projection of the arrangement of compounds (a) **1a** and (b) **1b**; corresponding Col_{ob} phase. Both the pink and green discs have small tilting (α) with respect to the disc normal, but the direction of tilt in the pink disc is just opposite to that of the green disc.

5. Photophysical Studies

a) Absorption and emission spectra in solution and thin-film state:

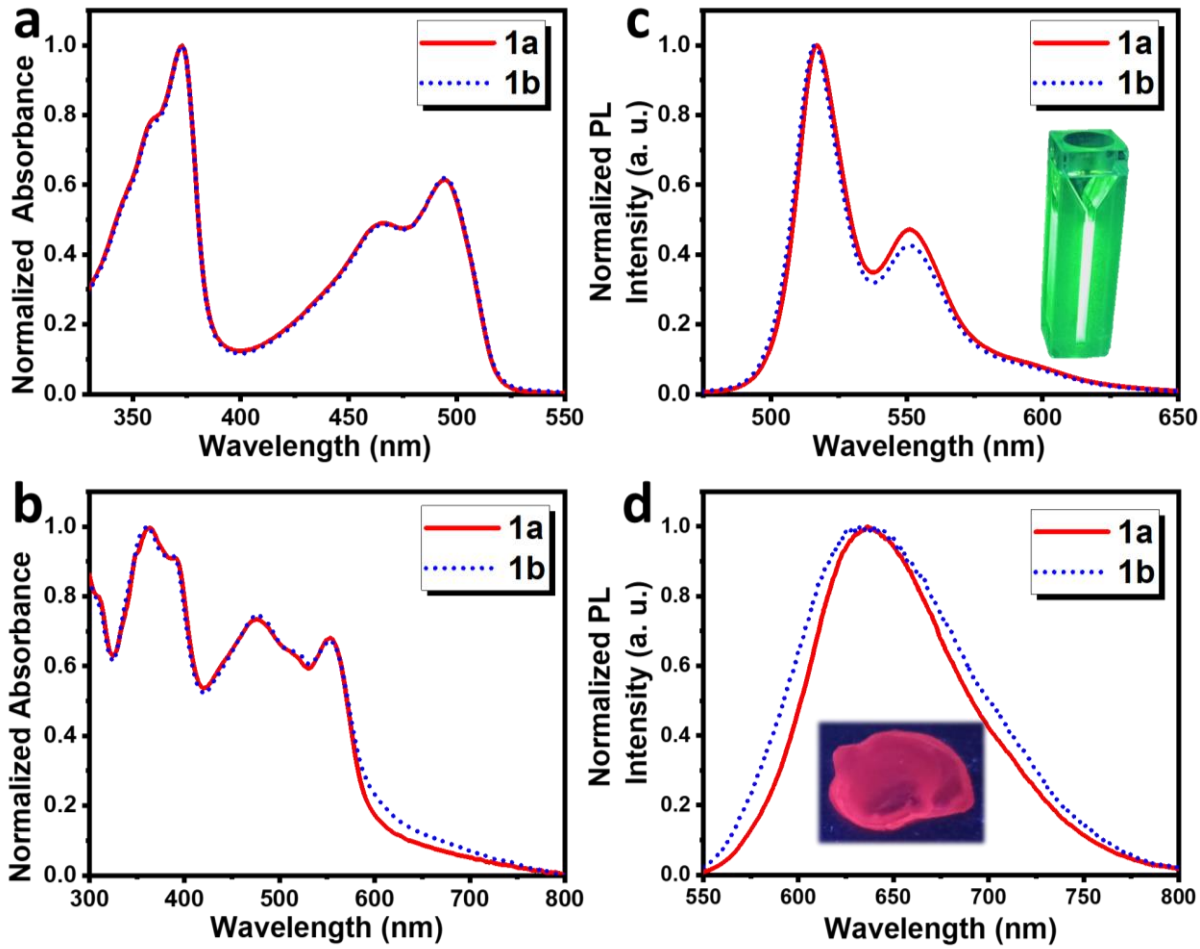

Figure S23: Normalized UV/Vis spectra in (a) solution state (10^{-6} M in THF) for **1a** and **1b** and (b) thin-film state for **1a** and **1b**. Normalized PL spectra in (c) solution state (10^{-6} M in THF) for **1a** and **1b** and (d) thin-film state for **1a** and **1b**.

Table S4: Photophysical data for mesogens **1a** and **1b**				
Mesogens	**UV/Vis**		**PL**	
	Absorbance peaks (nm)[a]	**Absorbance peaks (nm)[b]**	**Emission peaks (nm)[a]**	**Emission peak (nm)[b]**
1a	359, 373, 466, 494	363, 389, 476, 515, 553	517, 551	636
1b	361, 373, 466, 494	361, 386, 475, 513, 553	516, 551	631
[a]Recorded in 10^{-6} M THF solution. [b]Observed from the thin film.				

b) Concentration-dependent PL spectra

The basic characteristic of pyrene and its derivatives is their ability to generate an excimer. The data reveals that at low concentrations, the spectra have well-resolved peaks solely of emissions from the monomeric form in the yellowish-green region, and the diminishing of monomer emission begins in concentrated solutions. Also, the formation of excimer is evident from the appearance of the new additional broad and unstructured shoulder in the spectrum at higher wavelengths with increased concentration and subsequent fluorescence quenching. The relative intensity of the broad and red-shifted aggregated band (580-800 nm) in comparison to monomer emission increases as the concentration increases.

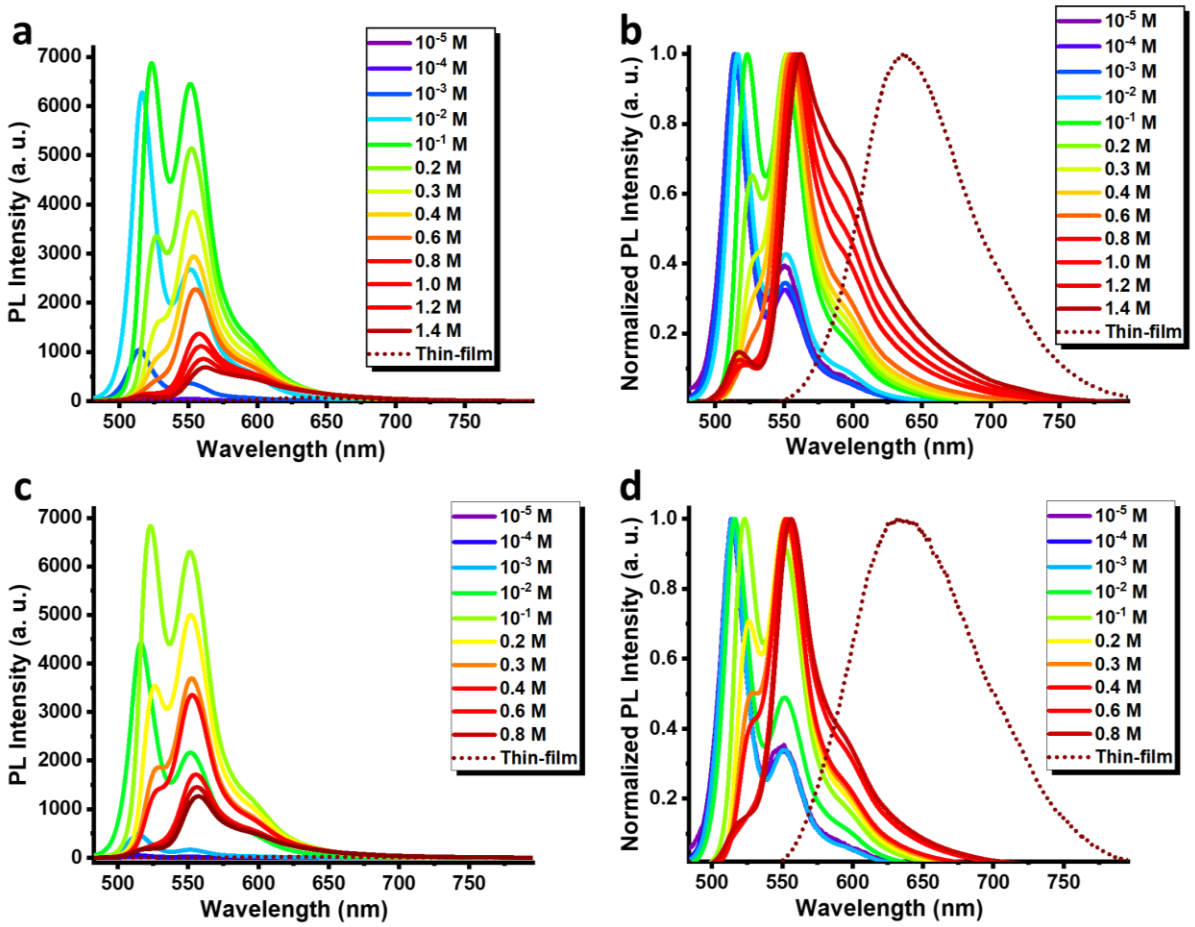

Figure S24: (a) Concentration-dependent PL spectra and (b) normalized concentration-dependent PL spectra for compound **1a**. (c) Concentration-dependent PL spectra and (d) normalized concentration-dependent PL spectra for compound **1b**.

6. Electrochemical Studies

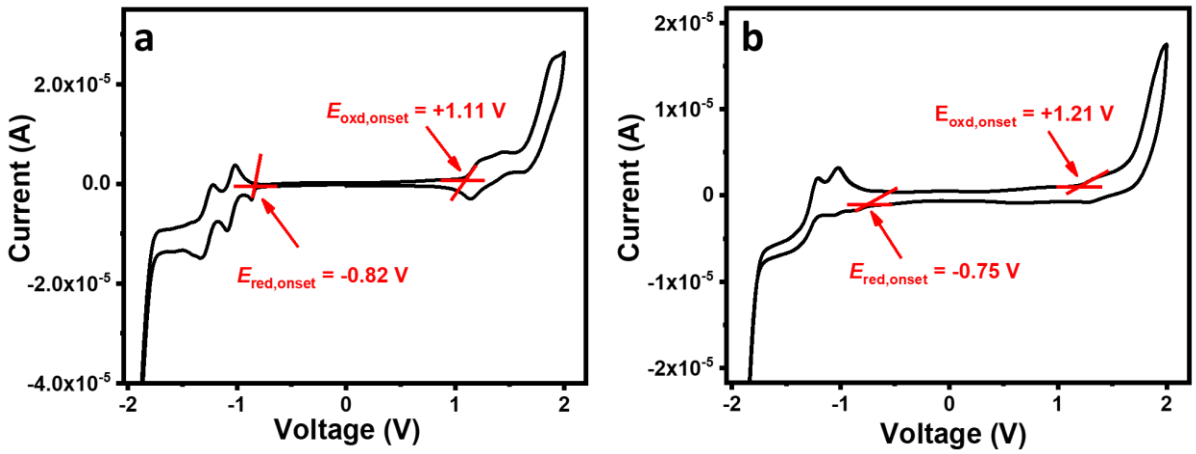

Figure S25. Cyclic voltammogram for compound (a) **1a** and (b) **1b**, at 50 mV s^{-1} scan rate. Experimental conditions: the reference electrode used - $Ag/AgNO_3$, the working electrode used - glassy carbon, the counter electrode used - platinum wire, and the supporting electrolyte used - 0.1 M tetrabutylammonium hexafluorophosphate.

Table S5: Electrochemical data for mesogens **1a** and **1b**

Mesogens	$E_{ox,onset}$ **(V)**	$E_{red,onset}$ **(V)**	E_{HOMO}[a] **(eV)**	E_{LUMO}[b] **(eV)**
1a	+1.11	-0.82	-5.37	-3.44
1b	+1.21	-0.75	-5.47	-3.51

[a]In dichloromethane, calculated from the oxidation onset ($E_{oxd,onset}$) of cyclic voltammogram as $E_{HOMO} = -[4.8 - E_{1/2,Fc/Fc^+} + E_{oxd,onset}]$ eV. [b]Calculated from the reduction onset ($E_{red,onset}$) of cyclic voltammogram, as $E_{LUMO} = -[4.8 - E_{1/2,Fc/Fc^+} + E_{red,onset}]$ eV, where $E_{1/2,Fc/Fc^+} = 0.54$ V.

7. DFT Studies

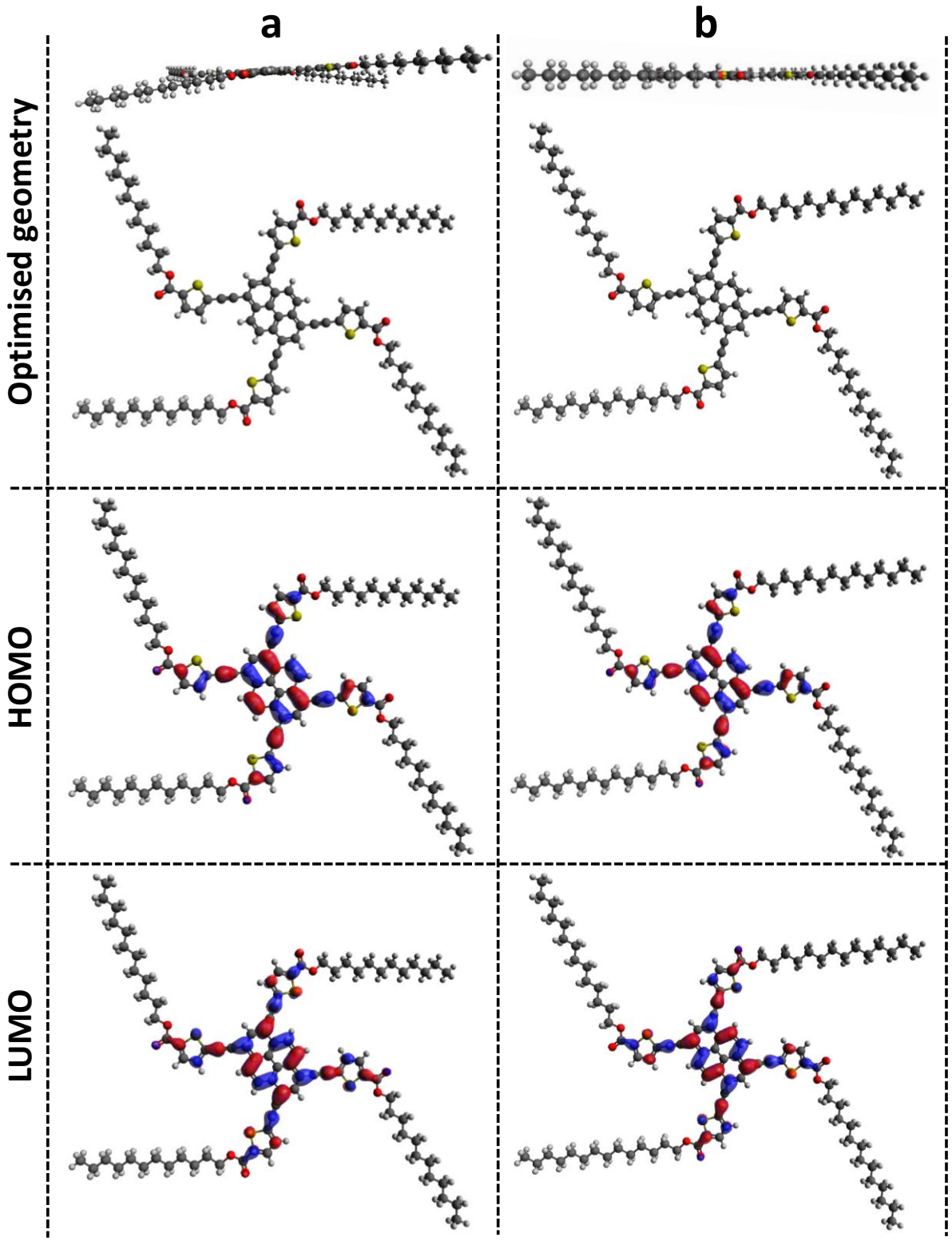

Figure S26. Frontier molecular orbitals electronic distribution of compound (a) **1a** and (b) **1b** using DFT/B3LYP/6-31G(d,p) method.[6,7]

8. Charge Carrier Mobility Studies

The charge carrier mobility measurements of compounds **1a** and **1b** were carried out using the ToF technique, outfitted with a Nd:YAG pulsed laser with a 5 ns pulse width and an excitation wavelength of 355 nm. The compounds were filled in ITO-coated sample cells of thickness 9.2 μm. The ToF measurements were carried out during cooling cycles that began with the compound's isotropic temperatures. During the measurements, the temperature of samples was controlled using a custom-made heating stage equipped with a EUROTHERM 3204 temperature controller.

Table S6. Hole mobility values of compounds **1a** and **1b** at different temperatures.

Compound	**Temperature / °C**	**μ_h / cm^2 V^{-1} s^{-1}**
1a	25	5.86×10^{-4}
	30	6.03×10^{-4}
	40	6.17×10^{-4}
	50	8.14×10^{-4}
	60	0.00135
	70	0.00164
1b	25	4.49×10^{-4}
	30	4.98×10^{-4}
	40	5.25×10^{-4}
	50	5.41×10^{-4}
	60	6.02×10^{-4}
	70	6.76×10^{-4}
	75	6.82×10^{-4}

The uncertainty in charge mobility values is about 10%, based on the assumed 10% uncertainty in the cell thickness and the sample's light penetration depth.

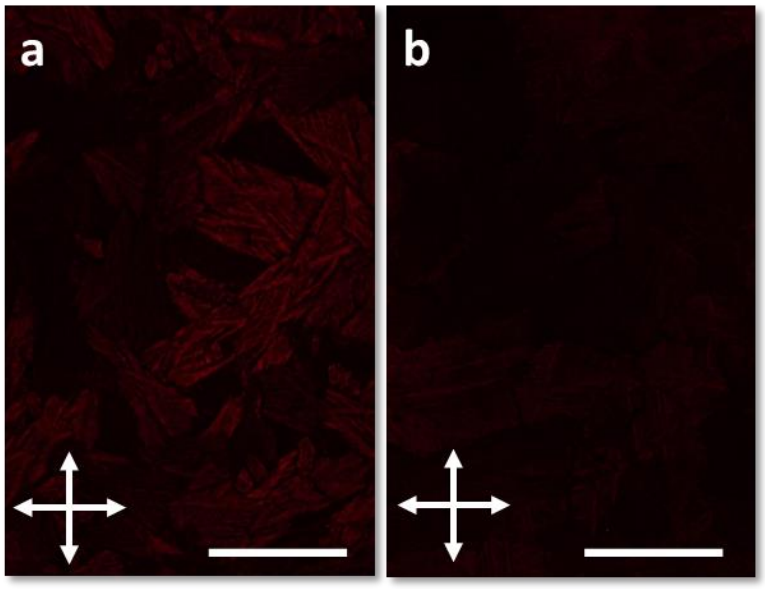

Figure S27: Photomicrographs of cells under a crossed polarizer for compounds (a) **1a** and (b) **1b** at room temperature (Scale bar = 100 µm).

9. Rheological Studies

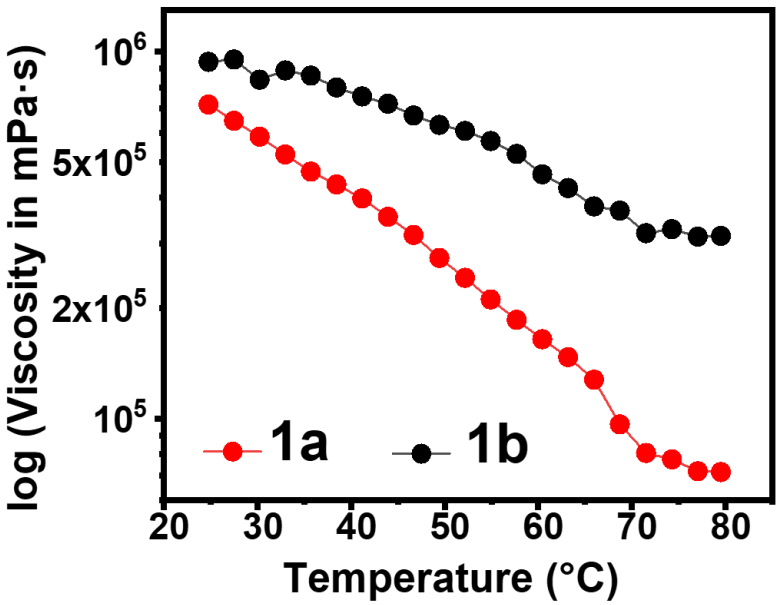

Figure S28. Temperature-dependent viscosity curve for compounds **1a** and **1b** on cooling from the isotropic phase.

10. References

1. S. Dhingra, I. Bala, J. De, S. P. Gupta, U. K. Pandey and S. K. Pal, *J. Mater. Chem. C*, 2021, **9**, 5628-5632.
2. S. Dhingra, I. Siddiqui, S. P. Gupta, Shahnawaz, J. Jayakumar, J.-H. Jou and S. K. Pal, *Soft Matter*, 2022, **18**, 8850-8855.
3. I. Bala, N. Singh, R. A. K. Yadav, J. De, S. P. Gupta, D. P. Singh, D. K. Dubey, J.-H. Jou, R. Douali and S. K. Pal, *J. Mater. Chem. C*, 2020, **8**, 12485-12494.
4. I. Bala, J. De, S. P. Gupta, H. Singh, U. K. Pandey and S. K. Pal, *Chem. Commun.*, 2020, **56**, 5629-5632.
5. T. Suzuki, Y. Ota, Y. Kasuya, M. Mutsuga, Y. Kawamura, H. Tsumoto, H. Nakagawa, M. G. Finn and N. Miyata, *Angew. Chem. Int. Ed.*, 2010, **49**, 6817-6820.
6. P. J. Stephens, J. F. Devlin, C. F. Chabalowski and M. J. Frisch, *J. Phys. Chem.*, 1994, **98**, 11623-11627.
7. A. D. Becke, *J. Chem. Phys.*, 1993, **98**, 5648-5652.